ACS APPLIED MATERIALS & INTERFACES

Research Article

Cite This: ACS Appl. Mater. Interfaces 2019, 11, 7148−7156

www.acsami.org

High-Fidelity Conformal Printing of 3D Liquid Alloy Circuits for Soft Electronics

Shuo Zhang,[†] Bei Wang,[†,‡] Jiajun Jiang,[†] Kang Wu,[†] Chuan Fei Guo,[§] and Zhigang Wu*[,†,‡]

[†]State Key Laboratory of Digital Manufacturing Equipment and Technology, Huazhong University of Science and Technology, Wuhan 430074, China

[‡]Department of Engineering Sciences, Uppsala University, Box 534, Uppsala 75121, Sweden

[§]Department of Materials Science and Engineering, Southern University of Science and Technology, Shenzhen 518055, Guangdong, China

Supporting Information

ABSTRACT: Owing to the great deformability from fluid, liquid alloy-based soft electronics has inherent advantages over rigid-based ones for applications such as stretchable intelligence or soft robotics, where high fidelity of three-dimensional (3D) conformability or dynamic morphology is required. However, current fabrications heavily rely on planar techniques, which severely limit their great potential in such attracting applications. By tuning the wettability of liquid alloy on a soft substrate through a selective surface morphology modification, we present a flexography printing technique of liquid alloy circuits on both planar (from diverse materials) and 3D complex surfaces and investigate the tuning mechanism and the relation between liquid alloy wettability and surface morphology modification. In a demonstration, high-fidelity printing of liquid alloy circuits can be deployed not only on the outline but also on small pits of strawberry surface, and the circuits work well in a dynamic deformation. Furthermore, being compatible with current industry process, our technique can be highly potential for future mass manufacturing of liquid alloy-based soft electronics.

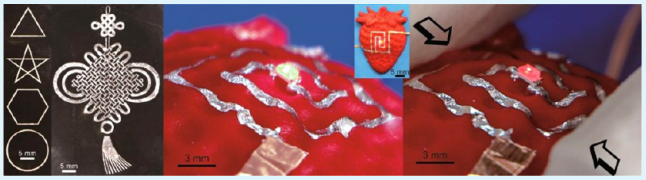

KEYWORDS: *wettability tune, flexography printing, liquid alloy, conformal printing, surface morphology control*

INTRODUCTION

Offering excellent mechanical compliance, soft/stretchable electronics paved a new way to make a new generation of human-intimated smart system, such as epidermal electronics[1] or soft robotics,[2] that can interact with people/external world without any obstructions, where smooth, soft, and ergonomic interfaces and designs are desired. To make such soft electronics, extensive studies have been carried out on different aspects, such as materials or mechanical design, in the past decades.[3−6] Among them, gallium liquid alloy-based soft electronics[7−9] or soft robotics[10,11] exhibit unique advantages in some aspects, such as high mechanical reliability (including self-healing after physical damage) and durability in bulk form,[12−14] high performance in stretchable radio frequency devices,[15−17] large areal stretchable electronics,[18] and new possibility of mono-integration of sense and actuation.[19] Technically, different fabrication techniques, such as capillary filling,[20−22] direct printing,[23,24] coflowed printing,[25] three-dimensional (3D) printing,[26−28] roller pen printing,[29,30] contact printing,[31] masked printing,[16,32] atomized printing,[33] freeze casting-assisted fabrication,[34] and laser-assisted printing,[35,36] have been demonstrated. Also, modifications of liquid alloy with interaction of metallic particles[37,38] and dispersing agents[39] have been investigated to enhance the printing quality or performance. However, most of the fabrication techniques are based on planar patterning techniques, which limit the great potential in applications in dynamic situations, such as interactive soft robotics, or complex surfaces, such as 3D conformal electronics.[40−44] Furthermore, although various fabrication techniques have been demonstrated, a technique compatible to current massively used techniques, such as flexography printing,[45,46] in today's press industry is not yet available to pattern liquid alloy circuits in a highly efficient way and to further fabricate corresponding soft devices conveniently.

In this work, we present an elegant approach to accomplish flexography printing with liquid alloy in a rapid way. By selectively modifying the morphology of a material matrix, we can tune the liquid alloy wettability on its surface and then selectively pattern liquid alloy on a UV-treated silicone stamp as a printing plate. Thus, by contacting the plate with liquid alloy and then transferring the liquid alloy onto a receiving/target substrate, we demonstrate a way of flexography printing of liquid circuits on the surfaces made from diverse material (Figure 1). Furthermore, thanks to the excellent compliance of silicone plate, the circuits can be directly printed onto a 3D complex surface conformably without any induced extra deformations

Received: November 22, 2018
Accepted: January 24, 2019
Published: January 24, 2019

DOI: 10.1021/acsami.8b20595
ACS Appl. Mater. Interfaces 2019, 11, 7148−7156

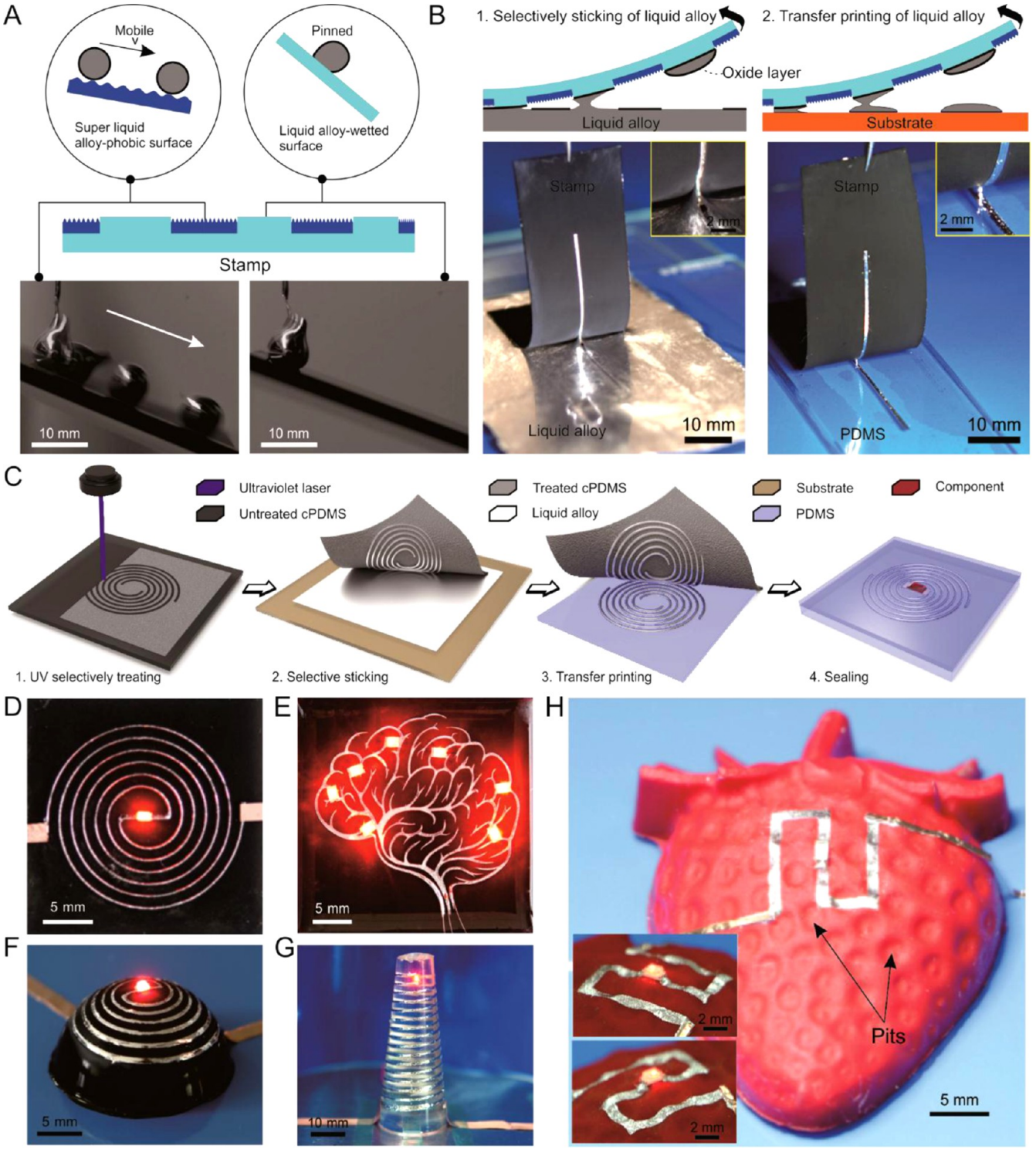

Figure 1. Wettability tuning-enabled flexography printing of liquid alloy circuits: principle, process, and application. (A) A selectively amphiphilic patterned plate for flexography printing of liquid alloy. Part of the plate is super liquid alloy-phobic, where liquid alloy cannot remain stable, while the other part is liquid alloy-philic, where liquid alloy can be well pinned. (B) Illustration and photographs of the major process of liquid alloy transferring during the printing—selectively sticking and transfer printing. (C) Brief illustration of the whole process of flexography printing. Several liquid alloy circuits demonstration based on our process. (D) A helix circuit of ~200 μm width on planar surface. (E) A tree with the shape of brain. (F) A helix circuit of ~1 mm on a semisphere surface. (G) A 3D liquid alloy circuit on the side surface of cone. (H) A liquid alloy circuit on a silicone strawberry surface with enlarged views. The depth and width of pits are ~1.3 and 1−2 mm, respectively.

(stresses) and corresponding long-term-induced fatigue or geometrical recovery.

Design of Liquid Alloy Flexography Printing. To achieve such kind of flexography printing of liquid alloy circuits, the most critical issue is to make an amphiphilic plate that can selectively attract printing ink, here liquid alloy, and then transfer it to receiving/target substrates, e.g., Ecoflex and poly(dimethylsiloxane) (PDMS). However, due to very high

DOI: 10.1021/acsami.8b20595
ACS Appl. Mater. Interfaces 2019, 11, 7148−7156

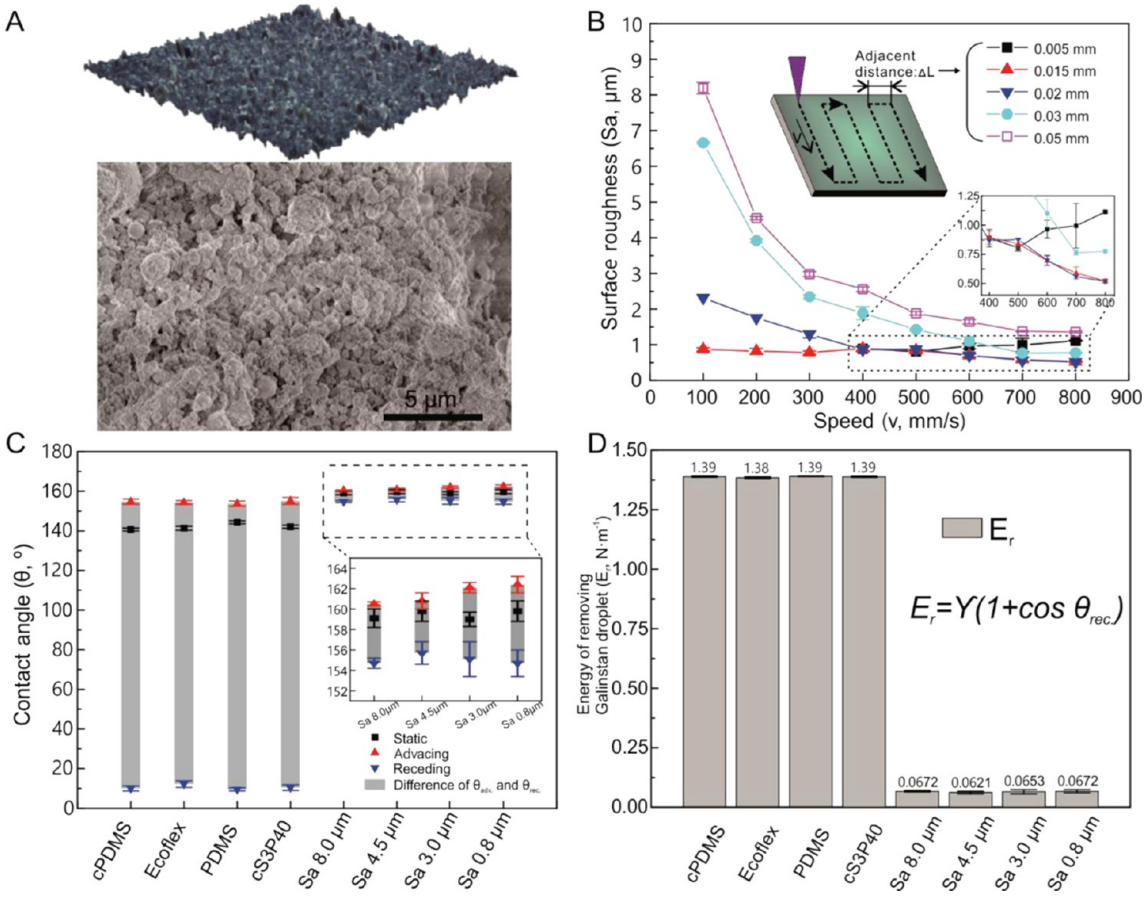

Figure 2. Surface morphology-tuned liquid alloy wettability on soft substrate. (A) An example of 3D morphology and scanning electron microscopy (SEM) image of super liquid alloy-phobic surface. (B) Surface roughness of UV-treated stamps with different scanning speeds (v) and interval of adjacent laser scanning lines (ΔL). (C) Contact angles (static angle, advancing angle, and receding angle) of liquid alloy droplet on different surfaces made from diverse materials. Sa (8.0, 4.5, 3.0, and 0.8 μm) indicates the surface roughness of treated cPDMS surface. (D) Calculated energy of removing liquid alloy droplet from different surfaces. The method of energy calculation is available in Supporting Note 1.

surface tension and existence of a thin solidlike oxide layer, gallium-based liquid alloy tends to be pinned onto many surfaces, even on those with very low surface energy such as silicones, as noticed in many previous works.[23,24,47,48] Hence, it is important to achieve a liquid alloy-phobic surface[49] or find a way that can selectively tune liquid alloy wettability on a surface. Even better, a super liquid alloy-phobic surface is favored (Figure 1A). Once upon touching the alloy-phobic area, the liquid alloy cannot remain there stably and will be repelled and then roll away (Figure S1 and Video S1) to liquid alloy-wetted area automatically. Consequently, a liquid alloy pattern is simultaneously obtained on the plate. By contacting and then removing from the receiving/target printing substrate, the liquid alloy pattern can be transferred onto the printing substrates (Figure 1B and Video S2). As disclosed by previous works on superhydrophobicity, one of the most effective ways to tune the surface properties is morphology control in micro/nanoscale.[50−54] In our demonstration, a UV laser marker is used to obtain such micro/nanosurface morphology of printing plate in a highly efficient way (Figure S2). Meanwhile, carbon-dosed silicone (cPDMS) is used to make printing stamp/plate, targeting to enhance the light absorbability. A brief illustration of our implementation is shown in Figure 1C. Inheriting high compliance from silicones, our technique can print not only complex liquid alloy circuits on planar surfaces, e.g., long curved line with a fixed line width and branched lines with varied widths in Figure 1D,E, but also three-dimensional developable/nondevelopable ones conformably (Figure 1F,G). Furthermore, thanks to the excellent compliance of silicone plate (cPDMS), high-fidelity printing on a three-dimensional complex surface with radical change rate of curvature, e.g., local small concaves on a large convex surface, can be achieved as well. In Figure 1H, such an example is demonstrated, where an light-emitting diode (LED) is connected by printed liquid alloy circuits on a silicone-replicated strawberry. The zoomed pictures from different perspectives indicate that the liquid alloy lines can faithfully follow the curvature of tiny pits (~1.3 mm in depth and 1−2 mm in width) on the surface without any observed gaps between the circuits and surface.

Liquid Alloy Wettability Tuning Study. According to Cassie's law, in an air environment, the contact angle (wettability) could be tuned by the area fraction of liquid alloy contacted with substrate and thus related to the roughness of the substrate (surface morphology). And in this study, surface morphology was directly modified by the UV laser. As shown in Figure 2A, there are micro/nanostructures on treated surface that can attract air effectively in the gaps, which decreases the effective contact area between liquid alloy oxide layer and treated surface, further preventing liquid alloy from being pinned on treated surface (liquid alloy-phobic surface). To learn more detailed information on how the UV laser can impact surface morphology, alloy wettability, and the corresponding

DOI: 10.1021/acsami.8b20595
ACS Appl. Mater. Interfaces 2019, 11, 7148−7156

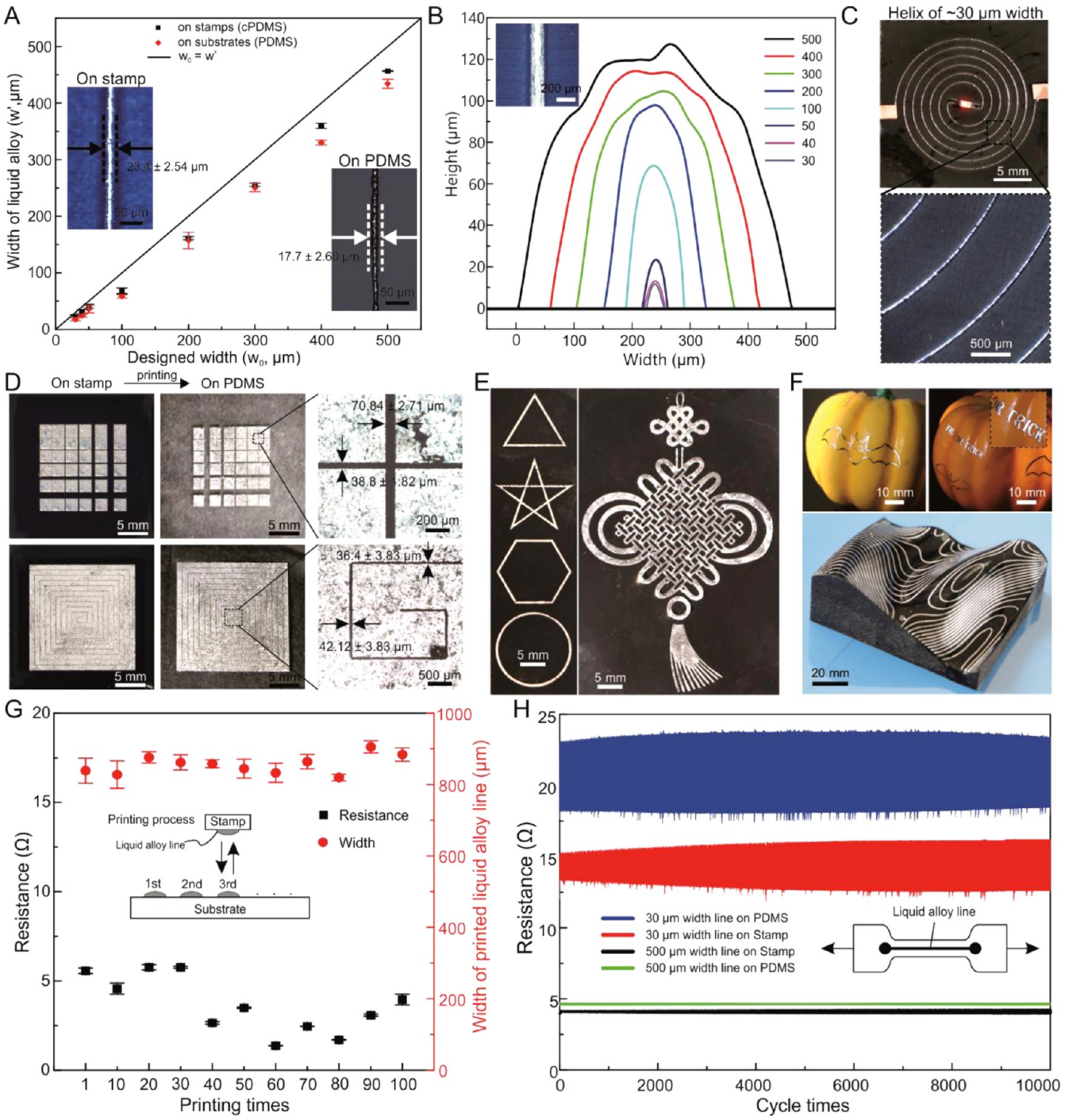

Figure 3. Patterning and characterization of flexography printing. (A) Designed and measured widths of liquid alloy lines on stamps/plates (UV-treated cPDMS) and receiving/target substrates (PDMS). The insets show a liquid alloy line with designed ~30 μm width on stamp and PDMS substrate. (B) Cross-sectional profile of liquid alloy lines ranging from 30 to 500 μm width on stamps/plates. The inset demonstrates a 200 μm wide line. (C) Photograph of a helical circuit (30 μm width) with a zoomed-in view. (D) Photographs of squares of 2 mm sides with spacing from ~50 to ~1000 μm on stamp/plate and PDMS substrate; the helix with spacing of ~40 μm on stamp/plate and PDMS. (E, F) Transferred patterns of polygons and a Chinese knot on planar surfaces, and bat, the word "TRICK" and contour lines on 3D complex surfaces (the maximum depth is 26.61 mm and the maximum curvature is 146.585 m^{-1}). (G) Measured width and electrical resistance of a liquid alloy line with a designed 1000 μm width during 100 times flexography printing on a planar surface. (H) Measured resistances of printed specimens during 10 000 times cycling test under a strain of up to 30%.

characterization and surface energy, we conducted a series of experiments. Technically, as shown in Figure 2B, the laser scanning speed and spatial density directly affect the final surface morphology, at a given laser power. As observed from the results in Figure 2B, surface roughness increased with much more spatial density (or smaller adjacent distance). On the condition that the adjacent distances (0.02, 0.03, and 0.05 mm) are not less than the width of laser facula (0.02 mm), with increase of scanning speed, the surface becomes smoother since the increased speed decreased the actual energy density transferred

DOI: 10.1021/acsami.8b20595
ACS Appl. Mater. Interfaces 2019, 11, 7148−7156

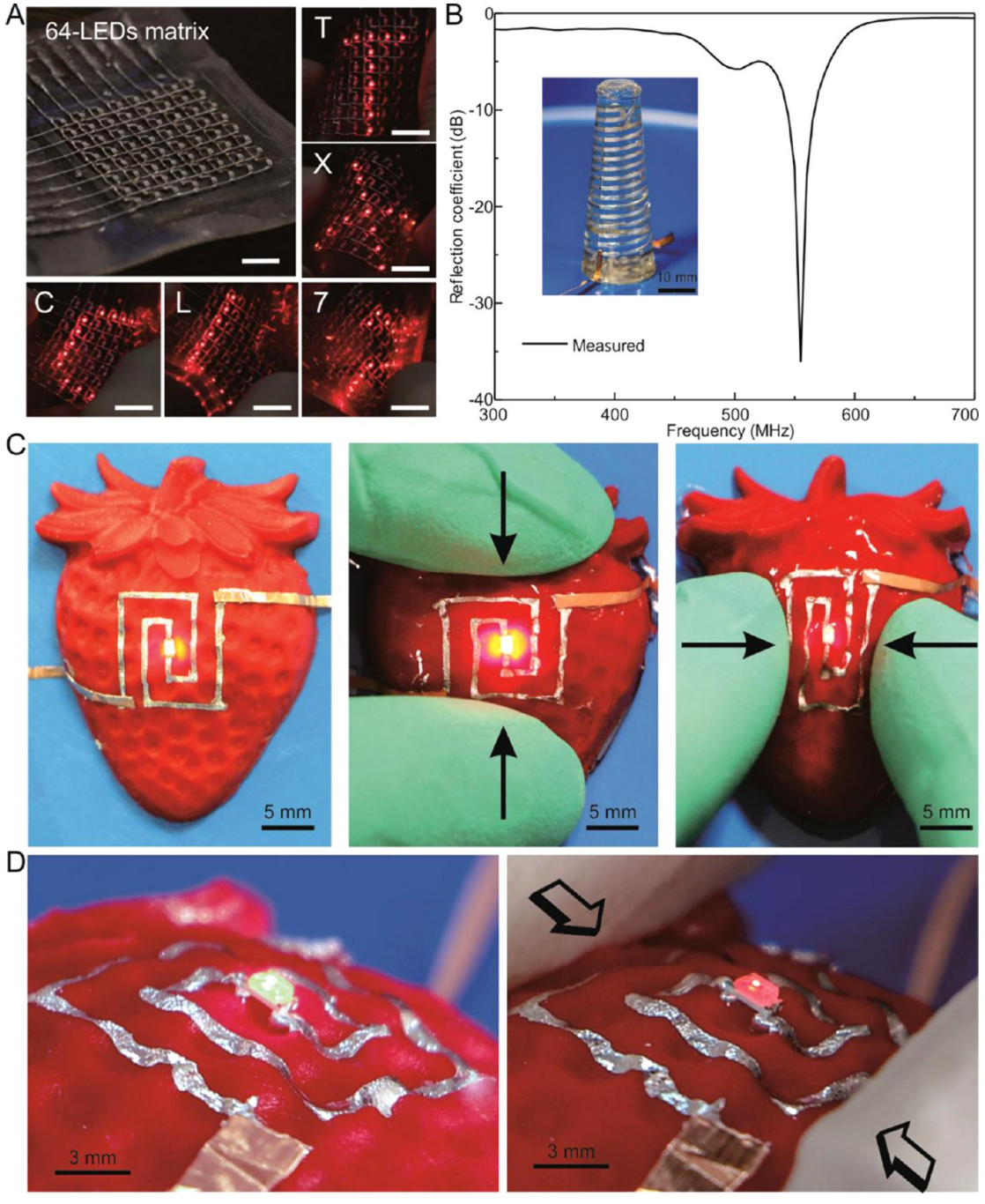

Figure 4. Application demonstrations of wettability tuning-enabled flexography printing from planar to 3D complex surfaces. (A) Photographs of a 64 LEDs array display during several arbitrary deformations. (B) Measured reflection coefficient of a 3D ellipse antenna printed on a three-dimensional developable surface. (C) Liquid alloy circuit on a three-dimensional nondevelopable complex surface — the surface of a strawberry under deformations, together with (D) enlarged views with/without mechanical deformation. More details are provided in Video S4. The depth and width of pits are ∼1.3 and 1−2 mm, respectively.

to the surface when laser power is fixed. However, on the condition that the adjacent distances (0.005 and 0.015 mm) are less than the width of laser facula (0.02 mm), there is little variation of roughness because the whole surface was completely ablated by laser.

According to the classical definition of superhydrophobicity, the measured static contact angle should be larger than 150°. In particular, high-quality superhydrophobicity often means small variation between advancing and receding contact angles. Referred to the above definition, we measured static, advancing, and receding contact angles of liquid alloy on the diverse treated surfaces (Figures 2C and S3). The static contact angles of UV-treated carbon-dosed PDMS (cPDMS) (∼160°) with different roughnesses (8.0, 4.5, 3.0, and 0.8 μm) are larger than that (∼144°) of untreated surfaces (cPDMS, Ecoflex, PDMS, and cS3P40). Noted that, the surfaces with/without laser treatment show very similar behavior, owing to the influence from naturally formed oxide layer. Huge differences appear to the variation of advancing and receding contact angles by comparing the surface with/without laser treatment. In particular, the differences of

DOI: 10.1021/acsami.8b20595
ACS Appl. Mater. Interfaces 2019, 11, 7148−7156

advancing angle ($\theta_{adv.}$) and receding angle ($\theta_{rec.}$) for UV-treated surfaces (within 8°) are significantly smaller than that (over 140°) for untreated surfaces, which refers to the fact that liquid alloy can easily be moved away from UV-treated surfaces but be pinned on untreated surfaces.

Furthermore, the receding angle could be used to calculate the energy of removing liquid alloy droplet from corresponding surfaces (1.38−1.39 N/m of untreated surfaces and (6.21−6.72) × 10^{-2} N/m of UV-treated surfaces) (Figure 2D) and the method in Supporting Note 1. The smaller the energy is, the more unstable is the liquid alloy droplet on the surface. All of these findings indicate that the liquid alloy is mobile on the UV laser-treated cPDMS and help obtain a sharp liquid alloy pattern on the plate, which guarantee printing quality in the following steps. In addition, for a specific roughed cPDMS, a higher roughness will bring better performance (although only a slight difference exists).

Liquid Alloy Patterning and Characterization. Using the new printing technique, we can achieve a robust line as narrow as ∼20 μm and a spacing line as ∼40 μm under current operating conditions (Figure 3). During the printing process, the liquid alloy is transferred first to the stamp/plate and then to the printing/target substrate. Such a double transfer process induces a minor variation of line width from designed to final ones on target substrate due to the influence of the laser facula-affected zone (Figure S4). To guide the practical operation from the designed lines to printed lines, we measured all of the three widths. Usually, the width on stamp is a bit narrower than that of the designed, while wider than that on printing/target substrate (Figures 3A and S5). Since a free liquid alloy reservoir is used in our experiments, the height of line increases along the increased width (Figure 3B). If necessary, a flat height of lines could be achieved by introducing a reservoir with limited height grids inside as that dose in the flexography printing used in press industry. Various patterns can be patterned on planar substrates, e.g., straight and curved lines in Figure 3C, array of squares with different spacing distances in Figure 3D, and different shapes such as triangles, stars, hexagon, circles, and even complex patterns such as Chinese knot in Figure 3E. Besides PDMS we demonstrated earlier, our printing technique can also work well on other printing/target substrates, e.g., Ecoflex, vinyl tape, glass, and polyester (Figure S6).

As mentioned above, due to excellent compliance of silicones, our printing technique can be used to a truly 3D conformal printing technique on both stiff and soft substrates, without introducing a dedicated 3D printer or advanced equipment and facility[40] (Figure 3F). With integrated components, such lines can be organized in a meaningful pattern to make a functional circuit/device as shown in Figure 3C. Furthermore, the printing plate/stamp can be reused many times. Without any specific optimizations, the plate can be reused more than 100 times with a small variation of printed line width (Figure 3G). Further, connecting with liquid alloy lines, which were printed by the stamp before and after 100 times usage, the LEDs could well function (Figure S7). In addition, our printed circuits exhibit excellent mechanical reliability when stretched. After 10 000 times cycles of stretching up to 30% strain, they still function very well (Figures 3H and S8).

Demonstrations. Besides one-layer printing, a multilayer (3D) soft device[55] can be achieved via our printing process in layer circuit stacking[18] by modifying our process slightly. As shown in Figure 4A, an array made of 64 LEDs can display any designed pattern, e.g., alphabets and numbers, under arbitrary deformations (Video S3). This feature may open a new way of dynamic interactions, e.g., to display information dynamically according to a real-time external mechanical stimulation (deformations). With a liquid alloy pattern printed on a spindle-shaped silicone, Figure 4B shows a well-functioned 3D ellipse antenna with a reflection coefficient of −36 dB at 555 MHz. To show high-fidelity conformability of our printing technique, a liquid alloy circuit is printed on a three-dimensional and nondevelopable surface of a silicone-replicated strawberry (Figure 4C,D and Video S4). According to the photographs, the liquid alloy circuits can be deployed not only on the outline but also on small pits of strawberry surface conformably in high fidelity, which is difficult to achieve with previously demonstrated stretchable electronics (Figure 4D and Video S4). Moreover, the fabricated devices function robustly before and after severe mechanical deformations, such as shaking, twisting, and squeezing (together with LED) or rubbing with a piece of fabric, being poked by a glass rod and wiped by a brush (Video S4).

Inheriting many features from flexography printing, our printing technique is also flexible in printing substrates (e.g., the ones in Figure S6) and production volume with necessary adaptations/automation to current industry facility, e.g., robot-assisted printing in Video S5. Besides this, our technique shows more advantages, e.g., 3D complex surface printing. The whole process major introduces a cost-effective UV laser marker (∼30 000 US dollar) used in a common laboratory environment, which indicates low equipment and facility investment. According to our situation, we estimate the processing time (Table 1). In a typical case for a planar printing (the processing time may vary with different situations), only 82 min is needed. Compared to many available techniques, it is a rather rapid process.

Table 1. Processing Time Estimation for a Typical Flexography Printing

processing steps	time (min)
pattern plotting[a,b]	20
cPDMS mixing	10
degassing	10
cPDMS curing	45
UV laser treating[c]	13
cutting and cleaning stamp	2
sticking and printing liquid alloy	2
total	82

[a]The process could be implemented as the same time as cPDMS mixing, degassing, and curing. [b]Time varies according to the complexity of the designed pattern. [c]This time was estimated on the condition that a stamp with an area of 40 mm × 40 mm was treated by the UV laser at a scanning speed of 400 mm/s and an adjacent distance of 0.005 mm.

CONCLUSIONS

In conclusion, by tuning the wettability of liquid alloy on a compliant surface via a UV laser selective roughening, we made a soft liquid alloy amphiphilic plate that can automatically form a liquid alloy pattern on the plate. With further transferring, complex liquid alloy circuits can be printed conformably on not only planar but also three-dimensional nondevelopable surfaces in high fidelity. It paves an efficient way to make liquid alloy-based soft electronic and smart systems in a massive way.

DOI: 10.1021/acsami.8b20595
ACS Appl. Mater. Interfaces 2019, 11, 7148−7156

MATERIALS AND METHODS

Printing Stamp/Plate Preparation. The stamp (carbon PDMS, cPDMS) was prepared via mixing PDMS (Sylgard 184, Dow Corning Corporation) of 10:1 g (silicone base/curing agent) with 0.2 g of carbon black (XC72R, CABOT) purchased from Alibaba. First, the carbon black and silicone base were stirred using a glass rod manually for 2−3 min following by digital stirring (RW 20, IKA, Germany) at ∼2000 rpm for 2−3 min. Second, the curing agent was added into the mixture by hand stirring for 2−3 min. After vacuumed for removing bubbles, the mixture was finally cured at 90 °C for 45 min in an oven (UF 55 plus, Memmert, Germany).

Printing Process and Characterization. As shown in Figure 1C, first, the stamp/plate (cPDMS) was selectively treated via a UV laser marker (HGL-LSU3/5EI, Huagong Laser, Wuhan, China) with pulse repetition frequency of 50 kHz, pulse width of 0.10 μs, and working current of 33.5 A. Second, after cleaning with isopropanol, the stamp/plate was placed on the liquid alloy (Galinstan, Geratherm Medical AG, Geschwenda, Germany) reservoir to selectively attract liquid alloy. Third, the stamp/plate carried with liquid alloy circuit was placed on the receiving/target substrate with slight pressure and then peeled off from it. Finally, the liquid alloy circuit was sealed with another layer of PDMS after component picked and placed if necessary. The photographs of the printing process shown in Figure 1B were taken with a camera (Canon EOS 70D, Tokyo, Japan), and the widths of the circuits were extracted from the photographs with a self-developed coded program in MATLAB (Version 2016b, MathWorks, Natick, MA).

Surface Characterization. The contact angles, including static and dynamic contact angles (advancing and receding angles) were measured by drop shape analysis equipment (DSA25, KRUSS, Germany) with the sessile drop method (Figures S2 and S3). The liquid alloy droplet was dropped on the tested surface via a syringe pump (PUMP 11 ELITE Nanomite, Harvard Apparatus, Holliston, MA) at room temperature. For dynamic contact angle measurement, both the advancing and receding speeds of increasing and decreasing liquid alloy droplet volumes were 4 μL/min. For static contact angle measurement, the volume of liquid alloy droplet was 6 μL. The behavior of liquid alloy droplet on different surfaces (Figures 1A, S1 and Video S1) was captured by a high-speed camera (Phantom V1212, Vision Research Inc.). The roughness of the modified super alloy-phobic surfaces (Figure 2A) was calculated by an ultradepth three-dimensional microscope (DSX 510, Olympus, Japan). Description of the detailed method of calculation can be found in Supporting Note 1. The surface morphologies of samples were characterized by SEM (Helios NanoLab G3 CX, FEI) (Figure 2B). The cS3P40 used in Figure 2C was obtained by mixing S3PDMS[56−58] (a soft, sticky, and stretchable PDMS-based elastomer) of 10 g silicone base, 1 g curing agent, and 40 μL PEIE (polyethylenimine ethoxylated, 80% ethoxylated solution 35−40 wt % in H_2O, MW 70 000 Sigma-Aldrich) with 0.2 g of carbon black.

Liquid Alloy Lines/Circuits Printing and Characterization. The stamps of printing liquid alloy lines with different widths (Figure 3A,D,G,H) were fabricated by the UV laser at a scanning speed of 400 mm/s and an adjacent distance of 0.005 mm. The profiles (including height and width) of liquid alloy lines were calculated by an ultradepth three-dimensional microscope (DSX 510, Olympus, Japan) (Figures 3A,D,G, S5, and S6). A dynamic mechanical test system (E1000, Instron, Boston) and a digital multimeter (34461A, Keysight Technologies) were used to carry out the 10 000 times cyclic test (Figures 3H and S8). The samples for cycling test (Figure S8) were cut by a cutoff knife with dimension of 4 mm × 75 mm (Kunshan Creator Testing Instrument Co. Ltd., China). The stamps/plates for printing liquid alloy circuit on 3D complex surfaces were obtained by mixing 50:1 g (silicone base/curing agent) of PDMS with 1.0 g of carbon black, which were ultrasoft to compliantly fit to 3D complex surfaces. All stamps for device fabricating were treated by the UV laser at a scanning speed of 400 mm/s and an adjacent distance of 0.005 mm. The fabrication for other demonstrations is slightly modified from the above protocols to adapt to different situations and can be found in Supporting Note 2.

Demonstration of Stamp/Plate Durability Testing. As shown in the inset of Figure 3G, the durability of stamp was tested by a process of sticking-printing liquid alloy line with designed 1000 μm width. Meanwhile, the resistances and widths of printed liquid alloy lines were measured by a multimeter (34461A, Keysight Technologies) and an ultradepth three-dimensional microscope (DSX 510, Olympus, Japan).

Characterization of Fabricated Devices. An array of 64 LEDs matrix is demonstrated in Figure 4A and Video S3, and the process details are illustrated in Figure S9. The fabrication process of 3D ellipse antenna is illustrated in Figure S10, and the reflection coefficient of the antenna was measured by a FieldFox handheld RF analyzer (N9914A, Keysight Technologies).

ASSOCIATED CONTENT

Supporting Information

The Supporting Information is available free of charge on the ACS Publications website at DOI: 10.1021/acsami.8b20595.

Liquid alloy droplet behavior on treated and untreated surfaces (MPG), a typical transfer printing process (MPG), a 64 LEDs matrix (MPG), 3D liquid alloy circuits under harsh conditions (MPG), and automatic process via a robot arm (MPG)

Energy calculation and detailed device fabrication, behavior of liquid alloy droplet on different surfaces, contact angles and microview characterization of super liquid alloy-phobic surface and liquid alloy-wetted surface, impact of laser facula-affected zone, printed liquid alloy lines, pattern "flexography" on various substrates, samples of cycling test, and illustrations of fabricating LEDs array and antenna and circuits (PDF)

AUTHOR INFORMATION

Corresponding Author

*E-mail: zgwu@hust.edu.cn, Zhigang.Wu@angstrom.uu.se.

ORCID

Chuan Fei Guo: 0000-0003-4513-3117

Zhigang Wu: 0000-0002-3719-406X

Author Contributions

Z.W. and S.Z. conceived the concept; Z.W., K.W., and S.Z. designed the experiments; and S.Z., B.W., and J.J. carried out experiments. All of the authors contributed to data analysis and manuscript preparation.

Notes

The authors declare no competing financial interest.

ACKNOWLEDGMENTS

The authors acknowledge the National Natural Science Foundation of China (Nos. U1613204 and 51575216) and Guangdong Innovative and Entrepreneurial Research Team Program (2016ZT06G587). Z.W. and C.F.G. acknowledge the support from Chinese government through its Thousand Youth Talents program.

REFERENCES

(1) Kim, D. H.; Lu, N.; Ma, R.; Kim, Y. S.; Kim, R. H.; Wang, S.; Wu, J.; Won, S. M.; Tao, H.; Islam, A.; Yu, K. J.; Kim, T. I.; Chowdhury, R.; Ying, M.; Xu, L.; Li, M.; Chung, H. J.; Keum, H.; McCormick, M.; Liu, P.; Zhang, Y. W.; Omenetto, F. G.; Huang, Y.; Coleman, T.; Rogers, J. A. Epidermal Electronics. *Science* **2011**, *333*, 838−843.

(2) Rus, D.; Tolley, M. T. Design, Fabrication and Control of Soft Robots. *Nature* **2015**, *521*, 467−475.

(3) Kim, D. H.; Rogers, J. A. Stretchable Electronics: Materials Strategies and Devices. *Adv. Mater.* **2008**, *20*, 4887−4892.

DOI: 10.1021/acsami.8b20595
ACS Appl. Mater. Interfaces 2019, 11, 7148−7156

(4) Rogers, J. A.; Someya, T.; Huang, Y. Materials and Mechanics for Stretchable Electronics. *Science* **2010**, *327*, 1603−1607.
(5) Fan, J. A.; Yeo, W.-H.; Su, Y.; Hattori, Y.; Lee, W.; Jung, S.-Y.; Zhang, Y.; Liu, Z.; Cheng, H.; Falgout, L.; Bajema, M.; Coleman, T.; Gregoire, D.; Larsen, R. J.; Huang, Y.; Rogers, J. A. Fractal Design Concepts for Stretchable Electronics. *Nat. Commun.* **2014**, *5*, No. 3266.
(6) Wang, C.; Wang, C.; Huang, Z.; Xu, S. Materials and Structures toward Soft Electronics. *Adv. Mater.* **2018**, *30*, No. 1801368.
(7) Cheng, S.; Wu, Z. Microfluidic Electronics. *Lab Chip* **2012**, *12*, 2782−2791.
(8) Wang, X.; Liu, J. Recent Advancements in Liquid Metal Flexible Printed Electronics: Properties, Technologies, and Applications. *Micromachines* **2016**, *7*, 206.
(9) Dickey, M. D. Stretchable and Soft Electronics Using Liquid Metals. *Adv. Mater.* **2017**, *29*, No. 1606425.
(10) Lu, N.; Kim, D. H. Flexible and Stretchable Electronics Paving the Way for Soft Robotics. *Soft Robot.* **2014**, *1*, 53−62.
(11) Rich, S. I.; Wood, R. J.; Majidi, C. Untethered Soft Robotics. *Nat. Electron.* **2018**, *1*, 102−112.
(12) Palleau, E.; Reece, S.; Desai, S. C.; Smith, M. E.; Dickey, M. D. Self-healing Stretchable Wires for Reconfigurable Circuit Wiring and 3D Microfluidics. *Adv. Mater.* **2013**, *25*, 1589−1592.
(13) Li, G.; Wu, X.; Lee, D.-W. A Galinstan-Based Inkjet Printing System for Highly Stretchable Electronics with Self-healing Capability. *Lab Chip* **2016**, *16*, 1366−1373.
(14) Markvicka, E. J.; Bartlett, M. D.; Huang, X.; Majidi, C. An Autonomously Electrically Self-Healing Liquid Metal−Elastomer Composite for Robust Soft-Matter Robotics and Electronics. *Nat. Mater.* **2018**, *17*, 618−624.
(15) Cheng, S.; Wu, Z. Microfluidic Stretchable RF Electronics. *Lab Chip* **2010**, *10*, 3227−3234.
(16) Jeong, S. H.; Hagman, A.; Hjort, K.; Jobs, M.; Sundqvist, J.; Wu, Z. Liquid Alloy Printing of Microfluidic Stretchable Electronics. *Lab Chip* **2012**, *12*, 4657−4664.
(17) Jobs, M.; Hjort, K.; Rydberg, A.; Wu, Z. A Tunable Spherical Cap Microfluidic Electrically Small Antenna. *Small* **2013**, *9*, 3230−3234.
(18) Cheng, S.; Wu, Z. Reversibly Stretchable, Large-Area Wireless Strain Sensor. *Adv. Funct. Mater.* **2011**, *21*, 2282−2290.
(19) Muth, J. T.; Vogt, D. M.; Truby, R. L.; Menguc, Y.; Kolesky, D. B.; Wood, R. J.; Lewis, J. A. Embedded 3D Printing of Strain Sensors Within Highly Stretchable Elastomers. *Adv. Mater.* **2014**, *26*, 6307−6312.
(20) Cheng, S.; Rydberg, A.; Hjort, K.; Wu, Z. Liquid Metal Stretchable Unbalanced Loop Antenna. *Appl. Phys. Lett.* **2009**, *94*, No. 144103.
(21) So, J.-H.; Thelen, J.; Qusba, A.; Hayes, G. J.; Lazzi, G.; Dickey, M. D. Reversibly Deformable and Mechanically Tunable Fluidic Antennas. *Adv. Funct. Mater.* **2009**, *19*, 3632−3637.
(22) Kubo, M.; Li, X.; Kim, C.; Hashimoto, M.; Wiley, B. J.; Ham, D.; Whitesides, G. M. Stretchable Microfluidic Radiofrequency Antennas. *Adv. Mater.* **2010**, *22*, 2749−2752.
(23) Zheng, Y.; He, Z.; Gao, Y.; Liu, J. Direct Desktop Printed-Circuits-on-Paper Flexible Electronics. *Sci. Rep.* **2013**, *3*, No. 1786.
(24) Boley, J. W.; White, E. L.; Chiu, G. T.-C.; Kramer, R. K. Direct Writing of Gallium-Indium Alloy for Stretchable Electronics. *Adv. Funct. Mater.* **2014**, *24*, 3501−3507.
(25) Wu, K.; Zhang, P.; Li, F.; Guo, C.; Wu, Z. On-Demand Multi-Resolution Liquid Alloy Printing Based on Viscoelastic Flow Squeezing. *Polymers* **2018**, *10*, 330.
(26) Ladd, C.; So, J.-H.; Muth, J.; Dickey, M. D. 3D Printing of Free Standing Liquid Metal Microstructures. *Adv. Mater.* **2013**, *25*, 5081−5085.
(27) Yu, Y.; Liu, F.; Zhang, R.; Liu, J. Suspension 3D Printing of Liquid Metal into Self-Healing Hydrogel. *Adv. Mater. Technol.* **2017**, *2*, No. 1700173.
(28) He, Y.; Zhou, L.; Zhao, H.; Gao, Q.; Fu, J.; Xie, C.; Liu, Y. Three-Dimensional Coprinting of Liquid Metals for Directly Fabricating Stretchable Electronics. *3D Print. Addit. Manuf.* **2018**, *5*, 195−203.
(29) Zheng, Y.; Zhang, Q.; Liu, J. Pervasive Liquid Metal Based Direct Writing Electronics with Roller-Ball Pen. *AIP Adv.* **2013**, *3*, No. 112117.
(30) Zheng, Y.; He, Z. Z.; Yang, J.; Liu, J. Personal Electronics Printing via Tapping Mode Composite Liquid Metal Ink Delivery and Adhesion Mechanism. *Sci. Rep.* **2014**, *4*, No. 4588.
(31) Tabatabai, A.; Fassler, A.; Usiak, C.; Majidi, C. Liquid-Phase Gallium-Indium Alloy Electronics with Microcontact Printing. *Langmuir* **2013**, *29*, 6194−6200.
(32) Kramer, R. K.; Majidi, C.; Wood, R. J. Masked Deposition of Gallium-Indium Alloys for Liquid-Embedded Elastomer Conductors. *Adv. Funct. Mater.* **2013**, *23*, 5292−5296.
(33) Jeong, S. H.; Hjort, K.; Wu, Z. Tape Transfer Atomization Patterning of Liquid Alloys for Microfluidic Stretchable Wireless Power Transfer. *Sci. Rep.* **2015**, *5*, No. 8419.
(34) Fassler, A.; Majidi, C. 3D Structures of Liquid-Phase GaIn Alloy Embedded in PDMS with Freeze Casting. *Lab Chip* **2013**, *13*, 4442−4450.
(35) Lu, T.; Finkenauer, L.; Wissman, J.; Majidi, C. Rapid Prototyping for Soft-Matter Electronics. *Adv. Funct. Mater.* **2014**, *24*, 3351−3356.
(36) Lu, T.; Markvicka, E. J.; Jin, Y.; Majidi, C. Soft-Matter Printed Circuit Board with UV Laser Micropatterning. *ACS Appl. Mater. Interfaces* **2017**, *9*, 22055−22062.
(37) Daalkhaijav, U.; Yirmibesoglu, O. D.; Walker, S.; Menguc, Y. Rheological Modification of Liquid Metal for Additive Manufacturing of Stretchable Electronics. *Adv. Mater. Technol.* **2018**, *3*, No. 1700351.
(38) Chang, H.; Guo, R.; Sun, Z.; Wang, H.; Hou, Y.; Wang, Q.; Rao, W.; Liu, J. Direct Writing and Repairable Paper Flexible Electronics Using Nickel-Liquid Metal Ink. *Adv. Mater. Interfaces* **2018**, *5*, No. 1800571.
(39) Mohammed, M. G.; Kramer, R. All-Printed Flexible and Stretchable Electronics. *Adv. Mater.* **2017**, *29*, No. 1604965.
(40) Adams, J. J.; Duoss, E. B.; Malkowski, T. F.; Motala, M. J.; Ahn, B. Y.; Nuzzo, R. G.; Bernhard, J. T.; Lewis, J. A. Conformal Printing of Electrically Small Antennas on Three-Dimensional Surfaces. *Adv. Mater.* **2011**, *23*, 1335−1340.
(41) Paulsen, J. A.; Renn, M.; Christenson, K.; Plourde, R. In *Printing Conformal Electronics on 3D Structures with Aerosol Jet Technology*, Proceedings of Future of Instrumentation International Workshop (FIIW), 8 to 9 October 2012; IEEE, 2012; pp 1−4.
(42) Vatani, M.; Engeberg, E. D.; Choi, J. W. Conformal Direct-Print of Piezoresistive Polymer/Nanocomposites for Compliant Multi-Layer Tactile Sensors. *Addit. Manuf.* **2015**, *7*, 73−82.
(43) Wang, X.; Zhang, Y.; Guo, R.; Wang, H.; Yuan, B.; Liu, J. Conformable Liquid Metal Printed Epidermal Electronics for Smart Physiological Monitoring and Simulation Treatment. *J. Micromech. Microeng.* **2018**, *28*, No. 034003.
(44) Tavakoli, M.; Malakooti, M. H.; Paisana, H.; Ohm, Y.; Marques, D. G.; Lopes, P. A.; Piedade, A. P.; Almeida, A. T.; Majidi, C. EgaIn-Assisted Room-Temperature Sintering of Silver Nanoparticles for Stretchable, Inkjet-Printed, Thin-Film Electronics. *Adv. Mater.* **2018**, *30*, No. 1801852.
(45) Kipphan, H. *Handbook of Print Media Technologies and Production Methods*; Springer Science & Business Media, 2001.
(46) Hösel, M.; Krebs, F. C. Large-Scale Roll-to-Roll Photonic Sintering of Flexo Printed Silver Nanoparticle Electrodes. *J. Mater. Chem.* **2012**, *22*, 15683−15688.
(47) Dickey, M. D.; Chiechi, R. C.; Larsen, R. J.; Weiss, E. A.; Weitz, D. A.; Whitesides, G. M. Eutectic Gallium-Indium (EGaIn): A Liquid Metal Alloy for the Formation of Stable Structures in Microchannels at Room Temperature. *Adv. Funct. Mater.* **2008**, *18*, 1097−1104.
(48) Joshipura, I. D.; Ayers, H. R.; Majidi, C.; Dickey, M. D. Methods to pattern liquid alloy. *J. Mater. Chem. C* **2015**, *3*, 3834−3841.
(49) Kadlaskar, S. S.; Yoo, J. H.; Abhijeet, J. J.; Lee, J. B.; Choi, W. Cost-Effective Surface Modification for Galinstan Lyophobicity. *J. Colloid Interface Sci.* **2017**, *492*, 33−40.
(50) Barthlott, W.; Neinhuis, C. Purity of the Sacred Lotus, or Escape from Contamination in Biological Surfaces. *Planta* **1997**, *202*, 1−8.

DOI: 10.1021/acsami.8b20595
ACS Appl. Mater. Interfaces 2019, 11, 7148−7156

(51) Feng, L.; Li, S.; Li, Y.; Li, H.; Zhang, L.; Zhai, J.; Song, Y.; Liu, B.; Jiang, L.; Zhu, D. Super-Hydrophobic Surfaces: from Natural to Artificial. *Adv. Mater.* **2002**, *14*, 1857−1860.
(52) Li, X.; Reinhoudt, D.; Crego-Calama, M. What Do We Need for A Superhydrophobic Surface? A Review on the Recent Progress in the Preparation of Superhydrophobic Surfaces. *Chem. Soc. Rev.* **2007**, *36*, 1350−1368.
(53) Roach, P.; Shirtcliffe, N. J.; Newton, M. I. Progess in Superhydrophobic Surface Development. *Soft Matter* **2008**, *4*, 224−240.
(54) Kramer, R. K.; Boley, J. W.; Stone, H. A.; Weaver, J. C.; Wood, R. J. Effect of Microtextured Surface Topography on the Wetting Behavior of Eutectic Gallium-Indium Alloys. *Langmuir* **2014**, *30*, 533−539.
(55) Huang, Z.; Hao, Y.; Li, Y.; Hu, H.; Wang, C.; Nomoto, A.; Pan, T.; Gu, Y.; Chen, Y.; Zhang, T.; Li, W.; Lei, Y.; Kim, N.; Wang, C.; Zhang, L.; Ward, J. W.; Maralani, A.; Li, X.; Durstock, M. F.; Pisano, A.; Lin, Y.; Xu, S. Three-Dimensional Integrated Stretchable Electronics. *Nat. Electron.* **2018**, *1*, 473−480.
(56) Jeong, S. H.; Zhang, S.; Hjort, K.; Hilborn, J.; Wu, Z. PDMS-Based Elastomer Tuned Soft, Stretchable, and Sticky for Epidermal Electronics. *Adv. Mater.* **2016**, *28*, 5830−5836.
(57) Adam, N. K.; Livingston, H. K. Contact angles and work of adhesion. *Nature* **1958**, *182*, 128.
(58) Kramer, R. K.; Boley, J. W.; Stone, H. A.; Weaver, J. C.; Wood, R. J. Effect of Microtextured Surface Topography on the Wetting Behavior of Eutectic Gallium-Indium Alloys. *Langmuir* **2014**, *30*, 533−539.

DOI: 10.1021/acsami.8b20595
ACS Appl. Mater. Interfaces 2019, 11, 7148−7156